

Synthesizing CT from Ultrashort Echo-Time MR Images via Convolutional Neural Networks

Snehashis Roy¹ *, John A. Butman², and Dzung L. Pham¹

¹ Center for Neuroscience and Regenerative Medicine, Henry Jackson Foundation,
USA

² Radiology and Imaging Sciences, Clinical Center, National Institute of Health, USA

Abstract. With the increasing popularity of PET-MR scanners in clinical applications, synthesis of CT images from MR has been an important research topic. Accurate PET image reconstruction requires attenuation correction, which is based on the electron density of tissues and can be obtained from CT images. While CT measures electron density information for x-ray photons, MR images convey information about the magnetic properties of tissues. Therefore, with the advent of PET-MR systems, the attenuation coefficients need to be indirectly estimated from MR images. In this paper, we propose a fully convolutional neural network (CNN) based method to synthesize head CT from ultra-short echo-time (UTE) dual-echo MR images. Unlike traditional T_1 -w images which do not have any bone signal, UTE images show some signal for bone, which makes it a good candidate for MR to CT synthesis. A notable advantage of our approach is that accurate results were achieved with a small training data set. Using an atlas of a single CT and dual-echo UTE pair, we train a deep neural network model to learn the transform of MR intensities to CT using patches. We compared our CNN based model with a state-of-the-art registration based as well as a Bayesian model based CT synthesis method, and showed that the proposed CNN model outperforms both of them. We also compared the proposed model when only T_1 -w images are available instead of UTE, and show that UTE images produce better synthesis than using just T_1 -w images.

1 Introduction

Accurate PET (positron emission tomography) image reconstruction requires correction for the attenuation of γ photons by tissue. The attenuation coefficients, called μ -maps, can be estimated from CT images, which are x-ray derived estimates of electron densities in tissues. Therefore PET-CT scanners are well suited for accurate PET reconstruction. In recent years, PET-MR scanners have become more popular in clinical settings. This is because of the fact that unlike CT, MRI (magnetic resonance imaging) does not impart any radiation, and MR images have superior soft tissue contrast. However, an MR image voxel contains

* Support for this work included funding from the Department of Defense in the Center for Neuroscience and Regenerative Medicine.

information about the magnetic properties of the tissues at that voxel, which has no direct relation to its electron density. Therefore synthesizing CT from MRI is an active area of research.

Several MR to CT synthesis methods for brain images have been proposed. Most of them can be categorized into two classes – segmentation based and atlas based. CT image intensities represent quantitative Hounsfield Units (HU) and their standardized values are usually known for air, water, bone, and other brain tissues such as fat, muscle, grey matter (GM), white matter (WM), cerebrospinal fluid (CSF) etc. Segmentation based methods [13,2] first segment a T_1 -w MR image of the whole head into multiple classes, such as bone, air, GM, and WM. Then each of the segmented classes are replaced with the mean HU for that tissue class, or the intensity at a voxel is obtained from the distribution of HU for the tissue type of that voxel.

Most segmentation based approaches rely on accurate multi-class segmentation of T_1 -w images. However, traditional T_1 -w images do not produce any signal for bone. As bone has the highest average HU compared to other soft tissues, accurate segmentation of bone is crucial for accurate PET reconstruction. Atlas based methods [6] can overcome this limitation via registration. An atlas usually consists of an MR and a co-registered CT pair. For a new subject, multiple atlas MR images can be deformably registered to the subject MR; then the deformed atlas CT images are combined using voxel based label fusion [3] to generate a synthetic subject CT. It has been shown that atlas based methods generally outperform segmentation based methods [6], because they do not need accurate segmentation of tissue classes, which can be difficult because it becomes indistinguishable from background, tissues with short T_1 , and tissues whose signal may be suppressed, such as CSF.

One disadvantage of registration based methods is that a large number of atlases is needed for accurate synthesis. For example, 40 atlases were used in [3], leading to significantly high computational cost with such a large number of registrations. To alleviate this problem, atlas based patch matching methods have been proposed [17,19]. For a particular patch on a subject MR, relevant matching patches are found from atlas MR images. The atlases only need to be rigidly registered to the subject [19]. The matching atlas MR patches can either be found from a neighborhood of that subject MR patch [19], or from any location within the head [17,16]. Once the matching patches are found, their corresponding CT patches are averaged with weights based on the patch similarity to form a synthetic CT. The advantage of patch matching is that deformable registration is not needed, thereby decreasing the computational burden and increasing robustness to differences in the anatomical shape. These type of methods also require fewer atlases (e.g., 10 in [19] and 1 in [17]).

Recently, convolutional neural networks (CNN), or deep learning [12], has been extensively used in many medical imaging applications, such as lesions and tumor segmentation [9], brain segmentation, image synthesis, and skull stripping. Unlike traditional machine learning algorithms, CNN models do not need hand-crafted features, and are therefore generalizable to a variety of problems. They

can accommodate whole images or much larger patches (e.g., 17^3 in [9]) compared to smaller sized patches used in most patch based methods (e.g., 3^3 in [19]), thereby introducing better neighborhood information. A CNN model based on U-nets [15] has been recently proposed to synthesize CT from T_1 -w images [5]. In this paper, we propose a synthesis method based on fully convolutional neural networks to generate CT images from dual-echo UTE images. We compare with two leading CT synthesis methods, one registration based [3] and one patch based [17], and show that our CNN model produces more accurate results compared to both of them. We also show that better synthesis can be obtained using UTE images rather than only T_1 -w images.

2 Data Description

MR images were acquired on 7 patients on a 3T Siemens Biograph mMR. The MR acquisition includes T_1 -w dual-echo UTE and MPRAGE images. The specifications of UTE images are as follows, image size $192 \times 192 \times 192$, resolution 1.56 mm^3 , repetition time $TR = 11.94\text{s}$, echo time $TE = 70\mu\text{s}$ and 2.46ms , flip angle 10° . MPRAGE images were acquired with the following parameters, resolution 1.0 mm^3 , $TR = 2.53\text{s}$, $TE = 3.03\text{ms}$, flip angle 7° . CT images were acquired on a Biograph 128 Siemens PET/CT scanner with a tube voltage of 120 kVp, with dimensions of $512 \times 512 \times 149$, and resolution of $0.58 \times 0.58 \times 1.5 \text{ mm}^3$. MPRAGE and CT were rigidly registered [1] to the second UTE image. All MR images were corrected for intensity inhomogeneities by N4 [20]. The necks were then removed from the MPRAGE images using FSL’s `robustfov` [7]. Finally, to create a mask of the whole head, background noise was removed from the MPRAGE using Otsu’s threshold [14]. UTE and CT images were masked by the headmask obtained from the corresponding MPRAGE. Note that the choice of MPRAGE to create the headmask is arbitrary, CT could also be used as well. The headmask was used for two purposes.

1. Training patches were obtained within the headmask, so that the center voxel of a patch contains either skull or brain.
2. Error metrics between synthetic CT and the original CT were computed only within the headmask.

3 Method

We propose a deep CNN model to synthesize CT from UTE images. Although theoretically the model can be used with whole images, we used patches due to memory limitations. Many CNN architectures have previously been proposed. In this paper, we adopt Inception blocks [18], that have been successfully used in many image classification and recognition problems in natural image processing via GoogleNet. The rationale for using this architecture over U-net is discussed in Sec. 5. The proposed CNN architecture is shown in Fig. 1.

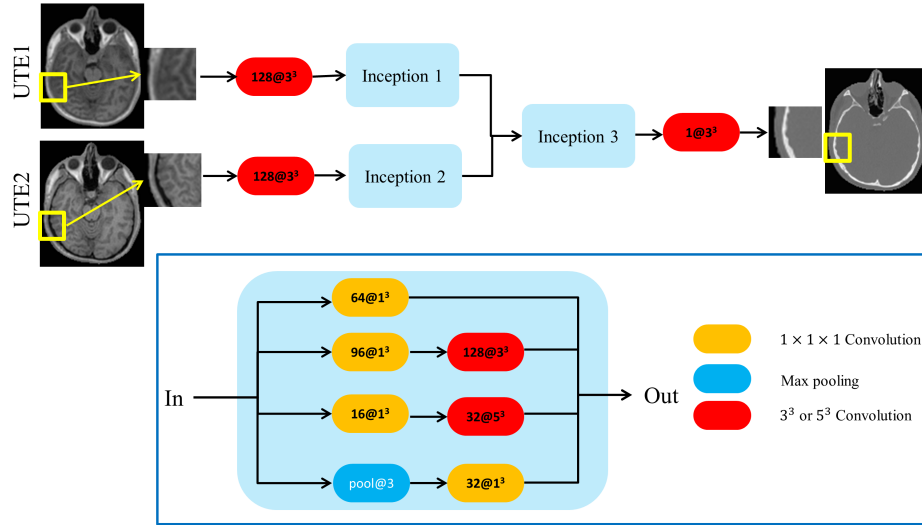


Fig. 1. The figure shows the proposed CNN model incorporating the Google Inception block [18], shown in inset. During training, patches from each of the dual-echo UTE images are first independently processed through two Inception blocks. Then their outputs are concatenated and again processed through another Inception block. Finally, the mean squared errors between the CT patch and the output of the third Inception block is minimized to train the parameters of the CNN. A convolution is written as $128@3^3$, indicating there are 128 filters of size $3 \times 3 \times 3$. The pooling layer is defined as $\text{pool}@3$, indicating maximum value within a $3 \times 3 \times 3$ region is used. Convolutions and pooling are done with stride 1. All convolutions are followed by ReLU, although for brevity, they are not shown here.

Convolutions and pooling are two basic building layers of any CNN model. Traditionally they are used in a linear manner, e.g. in text classification [11]. The primary innovation of the Inception module [18] was to use them in a parallel fashion. In an Inception module, there are two types of convolutions, one with traditional n^3 ($n > 1$) filter banks, and one with 1^3 filter banks. It is noted that 1^3 filters are downsampling the number of channels. The 1^3 filters are used to separate initial number of channels (128) into multiple smaller sets (96, 16, and 64). Then the spatial correlation is extracted via n^3 ($n > 1$) filters. The downsampling of channels and parallelization of layers reduce the total number of parameters to be estimated, which in turn introduces more non-linearity, thereby improving classification accuracy [4,18]. Note that the proposed model is fully convolutional, as we did not use a fully connected layer.

During training, $25 \times 25 \times 5$ patches around each voxel within the head-mask are extracted from the UTE images with stride 1. Then the patches from each UTE image are first convolved with 128 filters of size $3 \times 3 \times 3$. Such a filter is denoted by $128@3^3$ in Fig. 1. The outputs of the filters are processed

through separate Inception blocks. The outputs of these Inception blocks are then concatenated through their channel axis (which is same as the filter axis) and processed through another Inception block and a 3^3 filter. The coefficients of all the filters are computed by minimizing mean squared errors between the CT patch and the output of the model via stochastic gradient descent. Note that every convolution is followed by a ReLU (rectified linear unit), module, which is not shown in the figure. The pooling is performed by replacing each voxel of a feature map by the maximum of its $3 \times 3 \times 3$ neighbors.

We used Adam [10] as the optimizer to estimate the filter weights. Adam has been shown to produce much faster convergence than comparable optimizers. While training, we used 75% of the total atlas patches as training set and 25% as the validation set. To obtain convergence, 25 epochs were used. The filter parameters were initialized by randomly choosing numbers from a zero-mean Gaussian distribution with standard deviation of 0.001. A batch size of 64 was empirically chosen and found to produce sufficient convergence without requiring much GPU memory. The model was implemented in Caffe [8]. Anisotropic $25 \times 25 \times 5$ patches were used because larger size isotropic patches requires more GPU memory, while the patch size was empirically estimated. To compensate for the fact that patches are anisotropic, the atlas was reoriented in three different orientations – axial, coronal, and sagittal. Training was performed separately for each oriented atlas to generate three models, one for each orientation. Then for a new subject, the models were applied on the corresponding reoriented versions of the subject, and then averaged to generate a mean synthetic CT. Training on a TITAN X GPU with 12GB memory takes about 6 hours. Synthesizing a CT image from a new subject takes about 30 seconds, where approximately 10 seconds is needed to predict one orientation. Although the training is performed using $25 \times 25 \times 5$ patches, the learnt models are able to predict a whole 2D slice of the image by applying the convolutions on every slice. Each of the three learnt models were used to predict every 2D slice of the image in each of the three orientations. Then the 3 predicted images were averaged to obtain the final synthetic CT.

4 Results

We compared our CNN based method to two algorithms, GENESIS [17] and intensity fusion [3]. GENESIS uses dual-echo UTE images and generates a synthetic CT based on another pair of UTE images as atlases. While GENESIS is a patch matching method which does not need any subject to atlas registration, the intensity fusion method (called “Fusion”) registers atlas T_1 -w images to a subject T_1 -w image, and combines the registered atlas CT images based on locally normalized correlation. In our implementation of Fusion, the second echo of an UTE image pair was chosen as the subject image and was registered to the second echo UTE images of the atlases. The second echo was chosen for registration as its contrast closely matches the regular T_1 -w contrast used in [3].

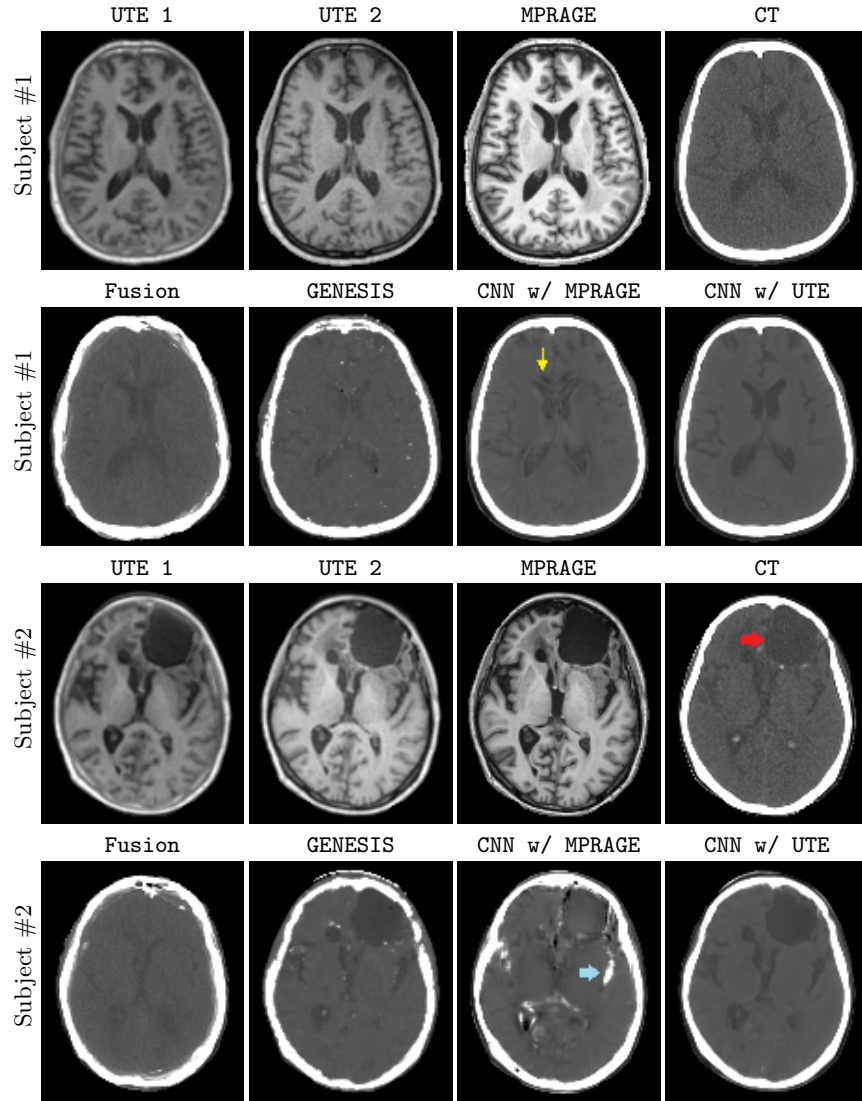


Fig. 2. Top two rows show UTE, MPRAGE, original, and synthetic CT images of a healthy volunteer. Bottom two rows show the same for a patient with a large lesion. Fusion [3] shows diffused bone in subject #1, while the CNN with MPRAGE shows some artifacts near ventricles (yellow arrow). Both GENESIS and the synthetic CT obtained with UTE can successfully reproduce the lesion (red arrow) for subject #2, with CNN synthesis showing less noise.

Similar to [5] which proposed a CNN model only using T_1 -w images, we also compared the proposed model with both channels as the MPRAGE.

Table 1. Quantitative comparison based on PSNR and linear correlation is shown for the competing methods on 6 subjects. Bold indicates largest value among the four synthetic CTs.

Metric	Method	Subject #					
		1	2	3	4	5	6
PSNR	Fusion	20.66	14.34	17.87	20.11	20.45	19.90
	GENESIS	18.89	16.28	17.20	17.96	21.52	21.17
	CNN w/ MPRAGE	22.35	16.46	16.00	22.06	21.91	21.32
	CNN w/ UTE	23.40	18.76	19.78	23.49	23.54	22.54
Correlation	Fusion	0.7377	0.6325	0.8097	0.7482	0.6807	0.6506
	GENESIS	0.5852	0.6800	0.7747	0.6277	0.6875	0.7132
	CNN w/ MPRAGE	0.7851	0.6995	0.6867	0.8007	0.7160	0.7137
	CNN w/ UTE	0.8384	0.8457	0.8820	0.8634	0.8174	0.8017

One patient was arbitrarily chosen to be the “atlas” for both GENESIS and the proposed CNN model with both UTE and MPRAGE as inputs. The trained CNN models are applied to the other 6 subjects. Since Fusion requires multiple atlas registrations, the validation is computed in a leave-one-out manner only for Fusion. GENESIS was also trained on the same atlas and evaluated on the remaining 6.

Fig. 2 shows examples of two subjects, one healthy volunteer and one with a large lesion in the left frontal cortex. For the healthy volunteer, all of the three methods perform similarly, while Fusion shows some diffused bone. It is because the deformable registrations can be erroneous, especially in presence of skull. CNN with MPRAGE shows some artifacts near ventricles (yellow arrow), while CNN with UTE images provide the closest representation to the original CT. For the subject with a brain lesion, Fusion can not successfully reproduce the lesion, as none of the atlases have any lesion in that region. CNN with MPRAGE shows artifacts where CSF is misrepresented as bone (blue arrow). This can be explained by the fact that both CSF and MPRAGE have low signal on MPRAGE. Synthetic CT from CNN with UTE shows the closest match to the CT, followed by GENESIS, which is noisier.

To quantitatively compare the competing methods, we used PSNR and linear correlation coefficient between the original CT and the synthetic CTs. PSNR is defined as a measure of mean squared error between original CT \mathcal{A} and a synthetic CT \mathcal{B} as, $PSNR = 10 \log_{10}(\frac{MAX_{\mathcal{A}}^2}{\|\mathcal{A}-\mathcal{B}\|^2})$, where $MAX_{\mathcal{A}}$ denotes the maximum value of the image \mathcal{A} . Larger PSNR indicates better matching between \mathcal{A} and \mathcal{B} . Table 1 shows the PSNR and correlation for Fusion, GENESIS, the proposed CNN model with only MPRAGE and with dual-echo UTE images. The proposed model with UTE images produces the largest PSNR and correlation compared to both GENESIS and Fusion, as well as CNN with MPRAGE. A Wilcoxon signed rank test showed a p-value of 0.0312 comparing CNN with UTE with the

other three for both PSNR and correlation, indicating significant improvement in CT synthesis. Note that we used only 6 atlases for our implementation of Fusion, although the original paper [3] recommended 40 atlases. Better performance would likely have been achieved with additional atlases. Nevertheless, the proposed model outperforms it with only one atlas.

5 Discussion

We have proposed a deep convolutional neural network model to synthesize CT from dual-echo UTE images. The advantage of a CNN model is that prediction of a new image takes less than a minute. This efficiency is especially useful in clinical scenarios when using PET-MR systems, where PET attenuation correction is immediately needed after MR acquisition. Another advantage of the CNN model is that no atlas registration is required. Although adding multiple atlases can increase the training time linearly, the prediction time (~ 30 seconds) is not affected by the number of atlases. This is significant in comparison with patch based [17,19] and registration based approaches [3] (~ 1 hr), where adding more atlases increases the prediction time linearly.

The primary limitation of the proposed, or in general, any CNN model is that it requires large amount of training data because the number of free parameters to estimate is usually large. In our case, by using only 3 Inception modules, the total number of free parameters are approximately 29,000. We used all patches inside the headmask which was about 500,000 for the 1.56 mm^3 UTE images. By adding more Inception modules, as done in GoogleNet [18], the number of free parameters grow exponentially, which needs more training data. An important advantage of the proposed model over the U-net in [5] is that only a single UTE image pair was used as atlas. Since we used patches instead of 2D slices [15,5] for training, the number of training samples is not limited by the number of slices in an atlas. One atlas with 256 slices was used to generate 500,000 training samples, which was sufficient to produce better results than competing methods. In clinical applications, it can be difficult to obtain UTE and high resolution CT images for many subjects. Therefore using patches instead of slices give exponentially more training samples.

The patch size ($25 \times 25 \times 5$) is an important parameter of the model which was chosen empirically to make best practical use of the available GPU memory. Although CNN models do not need hand-crafted features, it was observed that using bigger patches usually increases accuracy. However, there lies a trade-off between patch size and available memory. Future work includes optimization of patch size and number of atlases, as well as exploring further CNN architectures.

References

1. Avants, B.B., *et. al.*: A reproducible evaluation of ANTs similarity metric performance in brain image registration. *NeuroImage* 54(3), 2033–2044 (2011)

2. Berker, Y., *et. al.*: MRI-Based Attenuation Correction for Hybrid PET/MRI Systems: A 4-Class Tissue Segmentation Technique Using a Combined Ultrashort-Echo-Time/Dixon MRI Sequence. *Journal of Nuclear Medicine* 53(5), 796–804 (2012)
3. Burgos, N., *et. al.*: Attenuation correction synthesis for hybrid PET-MR scanners: Application to brain studies. *IEEE Trans. Med. Imaging* 33(12), 2332–2341 (2014)
4. Chollet, F.: Xception: Deep learning with depthwise separable convolutions. In: arXiv preprint arXiv:1610.02357 (2016)
5. Han, X.: MR-based synthetic CT generation using a deep convolutional neural network method. *Medical Physics* 44(4), 1408–1419 (2017)
6. Hofmann, M., *et. al.*: MRI-Based Attenuation Correction for Whole-Body PET/MRI: Quantitative Evaluation of Segmentation- and Atlas-Based Methods. *Journal of Nuclear Medicine* 52(9), 1392–1399 (2011)
7. Jenkinson, M., *et. al.*: FSL. *NeuroImage* 62(2), 782–790 (2012)
8. Jia, Y., *et. al.*: Caffe: Convolutional architecture for fast feature embedding. In: 22nd ACM Intl. Conf. on Multimedia. pp. 675–678 (2014)
9. Kamnitsas, K., *et. al.*: Efficient multi-scale 3D CNN with fully connected CRF for accurate brain lesion segmentation. *Medical Image Analysis* 36, 61–78 (2017)
10. Kingma, D.P., Ba, J.: Adam: A method for stochastic optimization. In: Intl. Conf. on Learning Representations (ICLR) (2015)
11. LeCun, Y., Bottou, L., Bengio, Y.: Gradient-based learning applied to document recognition. *Proc. IEEE* 86(11), 2278–2324 (1998)
12. LeCun, Y., *et. al.*: Deep learning. *Nature* 521(7553), 436–444 (2015)
13. Martinez-Moller, A., *et. al.*: Tissue Classification as a Potential Approach for Attenuation Correction in Whole-Body PET/MRI: Evaluation with PET/CT Data. *Journal of Nuclear Medicine* 50(4), 520–526 (2009)
14. Otsu, N.: A threshold selection method from gray-level histograms. *IEEE Trans. on Systems, Man, and Cybernetics* 9(1), 62–66 (1979)
15. Ronneberger, O., Fischer, P., Brox, T.: U-net: Convolutional networks for biomedical image segmentation. In: *Med. Image Comp. and Comp. Asst. Intervention (MICCAI)*. vol. 9351, pp. 231–241 (2015)
16. Roy, S., *et. al.*: MR to CT registration of brains using image synthesis. In: *Proc. of SPIE Med. Imaging*. vol. 9034, p. 903419 (2014)
17. Roy, S., *et. al.*: PET attenuation correction using synthetic CT from ultrashort echo-time MR imaging. *Journal of Nuclear Medicine* 55(12), 2071–2077 (2014)
18. Szegedy, C., *et. al.*: Going deeper with convolutions. In: Intl. Conf. on Comp. Vision. and Patt. Recog. (CVPR). pp. 1–9 (2015)
19. Torrado-Carvajal, A., *et. al.*: Fast patch-based pseudo-CT synthesis from T1-weighted MR images for PET/MR attenuation correction in brain studies. *Journal of Nuclear Medicine* 57(1), 136–143 (2016)
20. Tustison, N.J., *et. al.*: N4ITK: improved N3 bias correction. *IEEE Trans. Med. Imaging* 29(6), 1310–1320 (2010)